Journal of Molecular Structure 1024 (2012) 110–116

Contents lists available at SciVerse ScienceDirect

Journal of Molecular Structure

journal homepage: www.elsevier.com/locate/molstruc

Crystal structure, spectroscopy and theoretical studies of p-cyanobenzenosulfonamide and a Cu(II) complex

G.E. Camí [a], M.E. Chacón Villalba [b], P. Colinas [c], G.A. Echeverría [d], G. Estiu [e], D.B. Soria [b,*]

[a] Área de Química General e Inorgánica, Departamento de Química, Facultad de Química, Bioquímica y Farmacia, Universidad Nacional de San Luis, Chacabuco y Pedernera, 5700 San Luis, Argentina
[b] CEQUINOR, Departamento de Química, Facultad de Ciencias Exactas, Universidad Nacional de La Plata, 47 y 115, 1900 La Plata, Argentina
[c] LADECOR, Departamento de Química, Facultad de Ciencias Exactas, Universidad Nacional de La Plata, 47 y 115, 1900 La Plata, Argentina
[d] LANADI e IFLP (CCT-La Plata, CONICET), Departamento de Física, Facultad de Ciencias Exactas and Facultad de Ingeniería, Universidad Nacional de La Plata, CC67, 1900 La Plata, Argentina
[e] Department of Chemistry and Biochemistry, University of Notre Dame, Notre Dame, IN 46556, USA

HIGHLIGHTS

- p-Cyanobenzenosulfonamide and a new copper complex were prepared and characterized.
- The thermal behavior was investigated by thermogravimetric and differential thermal analysis.
- The experimental IR, Raman and UV–VIS spectra have been assigned using Density Functional (DFT) calculations at B3LYP/6-311+G** level.

ARTICLE INFO

Article history:
Received 29 February 2012
Received in revised form 1 May 2012
Accepted 2 May 2012
Available online 12 May 2012

Keywords:
p-Cyanobenzenosulfonamide
Cu(II) complex
Spectroscopic properties
X-ray structure
Density functional calculations

ABSTRACT

The results of the structural and electronic structure of p-cyanobenzenosulfonamide (L), and its copper(II) complex, $Cu(L)_2(NH_3)_2$ are reported. Both compounds have been prepared and their crystal structures determined. The sulfonamide crystallizes in the orthorhombic system, space group, Pnma and $Z = 4$, whereas the complex crystallizes in the triclinic system, P-1 and $Z = 2$. The coordination geometry of the copper(II) ion in the complex can be described as a distorted square planar with two N-sulfonamide and two NH_3 in opposite vertices. The thermal behavior of both, the ligand and the Cu(II) complex, was investigated by thermogravimetric analyses (TG) and differential thermal analysis (DT). The experimental IR, Raman and UV–VIS spectra have been assigned on the basis of DFT calculations.

1. Introduction

Sulfonamides are recognized for their antibacterial, antitumor, diuretic, antidiabetic, and antithyroid activity among others and are well known as carbonic anhydrase and protease inhibitors [1]. A new field of increasing interest in the last years is related to the use of metal based therapeutics for both diagnosis and treatment of diseases. The condensation products of sulpha drugs with aldehydes, ketones or their derivatives are very active biologically, besides having good complexing ability. Their activity, too, increases on complexation with metal ions. The most significant part of such metal based drug chemistry is, the ability of metal ions to bind in vivo with proteins and peptides [2]. Simple sulfonamides have been observed to attract much attention into this emerging area of metal based sulfa drugs, initially stimulated by the successful introduction of metal complexes of sulfadiazine to prevent bacterial infections [3]. Complexes based on sulfonamides as ligands are also artificial chemical nucleases that degrade DNA in the presence of sodium ascorbate. The interaction of these complexes with DNA has gained much attention due to possible applications as new therapeutic agents [4]. Thus, copper complexes are known to be promising reagents for the cleavage of nucleic acids [5].

In the light of the interest on coordination chemistry of sulfonamides, we report in the present study the synthesis of the p-cyanobenzenosulfonamide (L, in what follows) as well as its copper complex with formula $Cu(L)_2(NH_3)_2$. Their characterization by means of X-ray diffraction, thermogravimetry, IR, Raman, NMR and UV–VIS spectra is also discussed. The assignment of

* Corresponding author. Tel.: +54 221 4259485; fax: +54 221 4240172.
E-mail address: soria@quimica.unlp.edu.ar (D.B. Soria).

0022-2860/$ - see front matter © 2012 Elsevier B.V. All rights reserved.
http://dx.doi.org/10.1016/j.molstruc.2012.05.006

experimental electronic, infrared and Raman bands was accomplished with the aid of the theoretical results based in density functional theory.

2. Experimental

2.1. Material and methods

Chemical analyses for carbon, hydrogen and nitrogen were performed on 1108 elemental analyzer from Carlo Erba EA and copper content was determined by iodimetry. The FTIR spectra were carried out with an EQUINOX 55 spectrophotometer, in the range from 4000 to 400 cm^{-1} using the KBr pellet technique, with a spectral resolution of 4 cm^{-1}. The Raman spectra were recorded with a Bruker IFS 66 FTIR spectrophotometer provided with the NIR Raman attachment, with a resolution of 4 cm^{-1}. The electronic absorption spectra of the compounds were measured in two different conditions: on freshly prepared DMSO solutions in the 200–800 nm spectral range, and in solid state with KBr reference pellet. They were recorded with a Hewlett–Packard 8452-A diode array spectrometer, using 10 mm quartz cells. NMR spectra of p-cyanobenzenosulfonamide in DMSO-d_6 (purchased from Aldrich) solution was recorded on a Varian Mercury Plus, 200 MHz instrument at room temperature with TMS as an internal standard. DT and TG analyses were performed using Shimadzu TGA-50 and DTA-50H units at a heating rate of 5 °C min^{-1} and oxygen flow of 50 ml min^{-1}.

2.1.1. Synthesis of the p-cyanobenzenosulfonamide (**1**)

A cold solution of $NaNO_2$ (1.2 g, 17 mmol) was added to a suspension of sulfanilamide (2.5 g, 15 mmol) in 20 mL of a 2.3 N HCl solution at 0 °C with vigorous stirring. The resultant solution was poured into a suspension of KCN (4.16 g, 64 mmol) and $CuSO_4{\cdot}5H_2O$ (3.85 g, 15 mmol) in 20 mL of water. After stirring for 30 min, the solution was heated to 80 °C and then chilled. The precipitate was filtered, dried and extracted with 5% ethanol in benzene Soxhelt apparatus. The organic extract was concentrated and the solid recrystallized from water to afford p-cyanobenzenosulfonamide (1.6 g, 60%). m.p. 173.2 °C determined by thermogravimetry measures (TG-DT) and by melting point.

^{1}H NMR spectra: ^{1}H NMR: δ 7.58 (bs, –NH_2), 7.95 (d, J = 8.4 Hz, H-2, H-6), 8.06 (d, J = 8.4 Hz, H-3, H-5). ^{13}C NMR: δ 114.1 (C-4), 118.1 (–CN), 126.2 (C-2, C-6), 133.5 (C-3, C-5), 147.7 (C-1).

Analytical calculation for $C_7H_6N_2O_2S$ (%) C, 46.10%; H, 3.29%; N, 15.37%; found: C, 46.15%; H, 3.32%; N, 15.45%.

2.1.2. Synthesis of the [Cu(L)$_2$(NH$_3$)$_2$] complex (**2**)

The copper complex was prepared by direct reaction of ethanolic solutions of sulfonamide and copper(II) chloride in the 2:1 molar ratio, followed by drop wise addition of 0.6 ml of concentrated ammonia, under continuous stirring. The resulting mixture was stirred during ca. 4 h. and then was left to stand at room temperature. Slow evaporation of the solution provided well-developed violet crystals that were suitable for X-ray diffraction. They were collected by filtration washed and dried. The yield was 80%.

Analytical calculation for $C_{14}H_{16}CuN_6O_4S_2$ (%) C, 36.52%; H, 3.47%; N, 12.17%; found: C, 36.58%; H, 3.54%; N, 12.45%.

2.2. X-ray crystallography

Single-crystal X-ray data for compound **1** were taken on an automatic four-circle Enraf–Nonius CAD-4 diffractometer with graphite monochromated Cu Kα (λ = 1.54184 Å) radiation. The unit cell parameters and the orientation matrix for data collection were obtained from a least-squares refinement using the setting angles of 25 reflections in the θ range 14–45°. Data were collected at room temperature (293(2) K) in the ω–2θ scan mode up to θ_{max} = 70°, with scan rate ranging between 6.7 and 20° min^{-1}. Two standard reflections measured every 30 min were used to apply a decay correction (the maximum decay was 13%). The data collection and reduction were performed with the programs CAD-4 [6] and XCAD4 [7] respectively.

Data for complex **2** were obtained on an Oxford Xcalibur, Eos, Gemini CCD diffractometer with graphite-monochromated Cu Kα (λ = 1.54184 Å) radiation. X-ray diffraction intensities were collected (φ and ω scans with κ-offsets), integrated and scaled with the CrysAlisPro [8] suite of programs. The unit cell parameters were obtained by least-squares refinement based on the angular settings for all collected reflections using CrysAlisPro. Data were corrected empirically for absorption with CrysAlisPro.

The structures were solved by direct methods with SHELXS-97 and the molecular model refined by full-matrix least-squares procedure on F^2 with SHELXL-97 [9]. The crystallographic data, as well as additional details of data collection and refinement results for the two compounds are summarized in Table 1.

The programs SHELX [8], PLATON [10], PARST [11] and ORTEP-3 [12] within the WinGX packages [13] and MERCURY [14] were used for structure analysis and to prepare materials for publication.

In p-cyanobenzenosulfonamide compound, the hydrogen atoms were positioned stereo-chemically and refined with the riding model, while in the Cu(L)$_2$(NH$_3$)$_2$ complex they were located from the electronic Fourier different map and allowed to refine freely with the exception of the ammonia hydrogen atoms which were stereo-chemically located and refined by treating them as rigid bodies (allowing to rotate around the C–NH_3 bond).

Table 1
Crystal data, structure determination and refinement summary.

	(**1**)	(**2**)
Empirical formula	$C_7H_6N_2O_2S$	$C_{14}H_{16}CuN_6O_4S_2$
Formula weight	182.20	460.02
Temperature (K)	293(2)	293(2)
λ [Cu(Kα)] (Å)	1.54184	1.54184
Crystal system	Orthorhombic	Triclinic
Space group	Pnma	P-1
a (Å)	19.84(2)	6.2510(6)
b (Å)	7.826(1)	7.7440(8)
c (Å)	5.316(1)	10.6939(8)
α (°)	–	99.832(7)
β (°)	–	102.891(7)
γ (°)	–	104.892(8)
V (Å^3)	825.4(7)	473.16(8)
ρ_{calc} (g/cm^3)	1.466	1.614
Z	4	2
μ [Cu(Kα)] (mm^{-1})	3.178	4.001
F(000)	376	235
Crystal size (mm)	0.16 × 0.16 × 0.36	–
θ Range for data collection (°)	4.46–69.96	4.37–73.94
Limiting indices	$-24 \leqslant h \leqslant 24$	$-6 \leqslant h \leqslant 7$
	$-9 \leqslant k \leqslant 1$	$-9 \leqslant k \leqslant 9$
	$-6 \leqslant l \leqslant 0$	$-13 \leqslant l \leqslant 12$
Reflections collected	975	3548
Reflections unique with $I > 2\sigma(I)$	846	1911
Completeness to θ = 69.90°	99.6%	99.7%
Data/restraints/parameters	846/0/65	1911/0/148
Goodness-of-fit on F^2	1.090	1.036
R	0.0729	0.0444
R_w	0.1874	0.1125
$(\Delta/\rho)_{max}/(\Delta/\rho)_{min}$ (e/Å^{-3})	0.438/−0.405	0.504/−0.335

2.3. Computational methods

The computational study of the ligand and the copper complex were performed using the density functional theory (DFT) methods implemented in Gaussian 09 [15]. The systems studied herein were subjected to unrestrained energy minimizations using the B3LYP functional [16] with the 6-31+G** basis set [17] for nonmetal atoms and the Los Alamos effective core potentials LANL2DZ [18] for the metal. DFT methods have been shown to reproduce the structural properties of several biologically interesting transition metal centers, and their validity to model ground-state properties is widely accepted [19]. The basis sets were chosen as those that better reproduces the experimental UV–VIS data.

The geometry of the Cu-complex has been optimized in gas phase and both gas phase and DMSO modeled solvent were used for the optimization of the ligand. Their calculated spectral features were compared with experimental IR, Raman and UV–VIS data. The geometry optimized in gas phase has been used to calculate the IR frequencies, as they were determined in solid phase. IR frequencies have been corrected using 0.96 as scaling factor. The calculation of the UV–VIS spectra determined in solid phase was also based on the gas phase optimized geometry. In order to model the UV–VIS spectra experimentally determined in DMSO, the geometries were optimized modeling the solvent within a continuous approach (Polarizable Continuous Model, PCM) [20]. The same solvent model was used to calculate the UV–VIS spectra in DMSO. Time dependent DFT models were used in both cases in order to assign the nature of the observed electronic transitions.

2.4. CSD survey methodology

Version 5.31 of the CSD [21], containing 495,968 structures was used in this work. The complete CSD software system, which comprise Data base along with programs ConQuest [22] and Vista [23] were employed in the survey. We search structures containing at least one benzenosulfonamide derivative substituted in the *para* position with any substituent and bounded and not bounded to a transition metal atom through the amine nitrogen atom. The following filters were applied: error-free coordinates after CCDC in-house validation, no disorder, no powder studies and $R \leqslant 0.1$.

3. Results and discussion

3.1. Description of the crystal structure

System **1** crystallizes in the orthorhombic Pnma space group with four molecules in the unit cell located on the mirror plane (0,1,0). Fig. 1 shows the p-cyanobenzenosulfonamide molecule. The cyano group, the sulfonamide sulfur and the nitrogen atoms lie on the mirror plane and the six carbon ring planes been perpendicular to it. The amine hydrogen atoms of those molecules related by the diagonal glide plane (n) are pointing to the sulfonyl oxygen atoms connecting them through N–H···O short contacts (1.968 Å) as can be seen in Table 3. These contacts develop an extended two-dimensional hydrogen bonds network parallel to the (1,0,0) plane. On this plane the p-cyanobenzenosulfonamide molecules are arranged with their main molecular axis at an angle of 46.4(5)°. The cyano groups are antiparallely stacked along the b axis at a distance of 4.064(5)Å between two adjacent C–N bond centers. These arrangement allow short contact between a carbon ring hydrogen atoms (H13) and a cyano nitrogen atom and although this distance are rather long, intermolecular interaction via dipolar electric forces could not be ruled out.

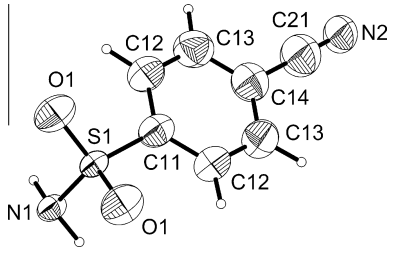

Fig. 1. Molecular plot of the p-cyanobenzenosulfonamide showing the labeling of the non-hydrogen atoms and their displacement ellipsoids at the 50% probability level.

Complex **2** crystallizes in the centrosymmetric triclinic space group P-1. The Cu(II) cation is located in a planar environment coordinated by two sulfonamide nitrogen atoms and two ammonia nitrogen atoms related by an inversion center. In Fig. 2 is shown the p-cyanobenzenosulfonamide molecules coordinated around the copper atoms and in Fig. 3a and b are plotted two view of its crystal packing. Along the b axis, sulfonamide groups of adjacent Cu(II) cations are linked by centrosymmetric cyclic dimer of N–H···O contacts, involving the amine hydrogen atom H1 and oxygen atom O1. The cyclic dimer plane and that one formed by the atoms coordinated to Cu(II) cations lie approximately on the same layer parallel to the (−1,0,3) plane. On this layer, another four inversion related N–H···O contacts are observed (see Fig. 3a). Two of them link the ammonia hydrogen atom H31 with the oxygen atom O2 of sulfonamide groups bounded to the same Cu(II) cation, whereas the other two link the ammonia hydrogen atom H33 with the oxygen atom O1 of sulfonamide groups bounded to Cu(II) cations related by inversion centers (see Fig. 3a). These layers are connected also by N–H···O contacts involving the ammonia hydrogen atom H32 and the sulfonamide oxygen atom O2, developing a corrugated two-dimensional network of N–H···O contacts parallel to the (0,0,1) layer, as can be seen in Fig. 3a. Finally, these layers are connected by C–H···N contacts involving the ring carbon hydrogen atom H13 and the cyanide nitrogen atom N2 (see Table 3 and Fig. 3b).

A comparison of the p-cyanobenzenosulfonamide molecule in **1** with that bound to Cu(II) cation in **2** shows that sulfonamide group are differently orientated with respect to the molecular ring plane, the C12–C11–S1–N1 torsional angles are 88.7(3)° and 37.9(3)° respectively. In addition, in **2** the N1–S1 distance is shorter, while the S1–O1 and S1–O2 distances are longer than those observed in **1** (Table 2). The comparison of the calculated mean bond distances in 14/90 sulfonamide groups bounded/not bounded to a transition metal atom obtained from a search in the CSD [21], S–N = 1.5804/1.6039, S–O = 1.4421/1.4350 and S–O′ = 1.4429/1.4351 Å respectively, shows a similar behaviour of the sulfonamide group. These results suggest a partial charge transfer after deprotonation from the amine nitrogen atom to the sulfonyl S1–N1 bond, increasing its S1–N1 bond order while decreasing the S–O double bonds character.

3.2. Thermogravimetric study

3.2.1. TG-DT of the ligand

The thermogravimetric curve shows that the ligand is stable up to 230 °C. Two sharp loss of weight of 58.6% (23% and 35.16%) take place in the 200–360 °C temperature range, probably due to the evolution of those coordinated to the benzene as sulfonamide and CN groups (expected 58%). The third step occur with a weight loss of 41.4% ending at 500 °C. This is probably due to decomposition of the benzene ring (expected 41.8%).

The DT curve shows and endothermic processes at approximately 172.9 °C, without weight loss in the TG curve corresponding to the melting point.

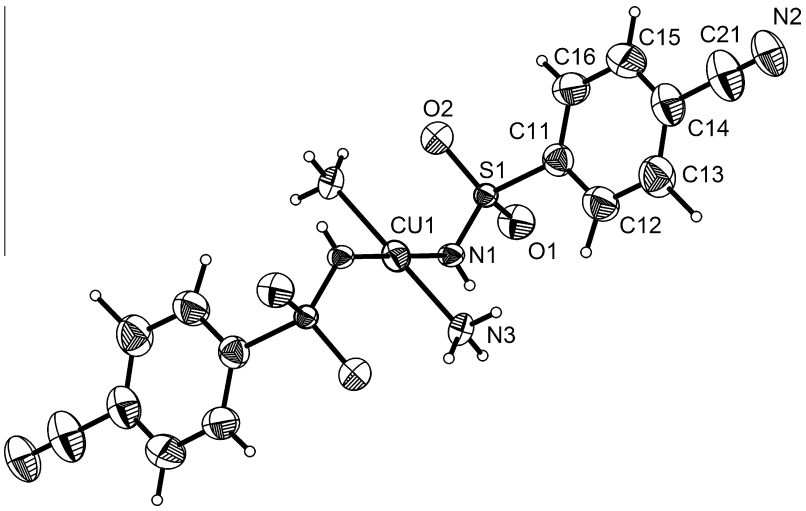

Fig. 2. Molecular plot of the p-cyanobenzenosulfonamide copper complex.

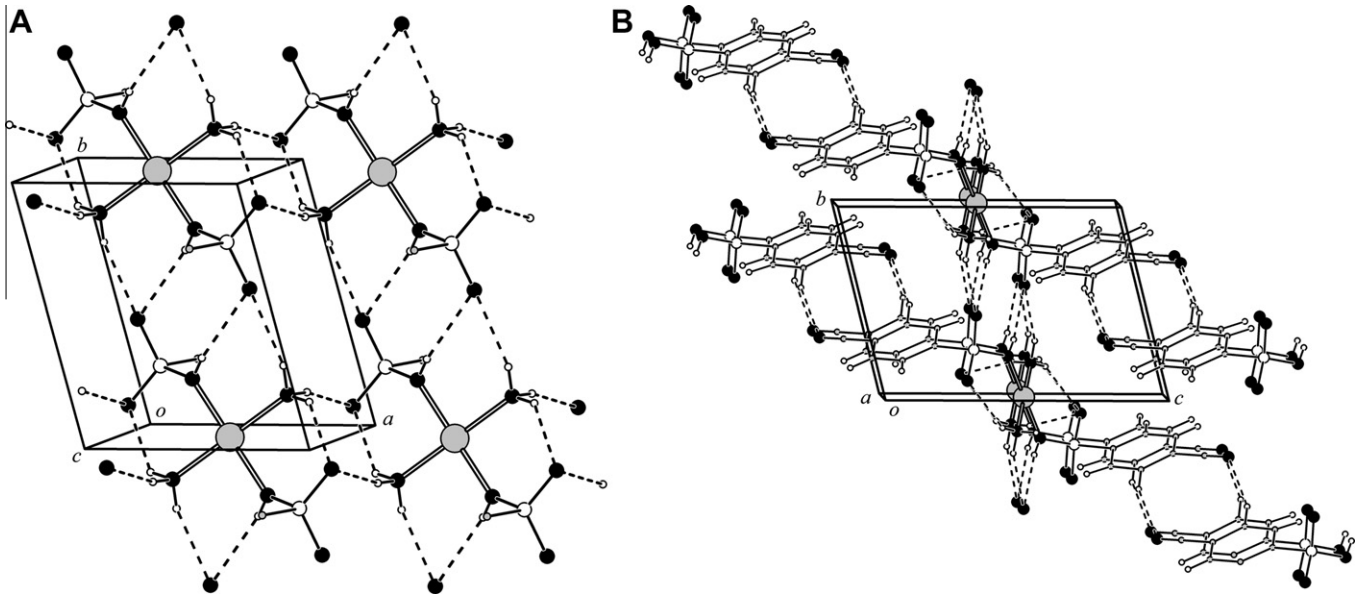

Fig. 3. (a) Projection of the p-cyanobenzenosulfonamide copper complex down the crystal *a*-axis. (b) Diagram showing the corrugated N–H···O contacts layer. For clarity, benzene moiety and cyano group are not included. Contacts are represented in dashed lines.

Two endothermic peaks are observed at 298 and 322 °C due to the coordinated groups. Finally and endothermic one with maximum at 550 °C is also displayed.

3.2.2. TG-DT of the complex

The TG curve of the complex reveals that the decomposition takes place in three steps. The two first ones correspond to a weight loss of 6.82% which is consistent with the evolution of the two NH_3 groups (loss of weight calculated 7.30%). These process take place with two endothermic peaks observed in DT curve at 137 °C and 186 °C. The third step occurs with a weight loss of 52.73% corresponding to the decomposition of the benzene ring and the coordinated groups as CN and NH (loss of weight calculated 51.52%). This value may be assigned to the reaction of the SO_2 group with Cu and a partial oxidation to cupric sulfate, as observed in the infrared spectra of the residue. This fact was also observed in a thermogravimetric study of the sulfonamide copper complexes [24,28]. The DT curve shows three exothermic peaks at 178, 190 and 214 °C corresponding to the partial decomposition of the ligand. A second group of exothermic peaks is observed at 375, 384, 389 and 409 °C, and corresponds to the complete decomposition of the ligands and to the oxidation process described for the TG curve interpretation.

3.3. Spectroscopic properties

3.3.1. IR and Raman spectra

The observed Raman and FTIR bands of the p-cyanobenezenosulfonamide (1) and its Cu(II) complex (2) are shown in Fig. 4 and the most significant experimental and calculated frequencies are given in Table 4. The spectrum of the complex was compared with the one of the free sulfonamide in order to determine the coordination sites that may be involved in chelation. It was also compared with those of previously reported similar complexes [24–32].

The most remarkable difference is noticed in the band corresponding to the sulfonamide stretching vibrations. The FTIR spectrum of the ligand (1) shows bands at 3350–3250 cm^{-1} and at

Table 2
Selected bond distances (Å), bond angles (°), and torsional angles (°) for ligand (1) and complex (2).

Parameter	1		2	
	Exp.	Calc.	Exp.	Calc.
Cu1–N1	–	–	1.983(2)	1.991
Cu1–N3	–	–	2.002(3)	2.074
S1–O1	1.420(2)	1.463	1.449(2)	1.472
S1–O2	–	1.463	1.445(2)	1.486
S1–N1	1.601(3)	1.677	1.554(2)	1.619
C11–S1	1.777(4)	1.809	1.788(3)	1.815
C11–C12	1.377(3)	1.397	1.375(4)	1.398
C12–C13	1.386(5)	1.393	1.387(4)	1.393
C13–C14	1.383(4)	1.406	1.388(5)	1.406
C14–C21	1.461(7)	1.436	1.450(4)	1.436
C21–N2	1.129(6)	1.163	1.123(5)	1.164
N1–Cu1–N3	–	–	88.7(1)	88.54
C11–S1–O1	107.4(1)	106.9	105.1(1)	104.9
N1–S1–O1	106.6(1)	105.6	110.9(1)	107.2
N1–S1–C11	108.7(2)	107.3	109.5(1)	107.9
O1–S1–O1 or O2	119.6(2)	123.5	115.4(1)	119.9
C12 or C16–C11–C12	122.5(4)	119.2	120.9(3)	119.6
C12–C11–S1	118.7(2)	119.1	119.9(2)	119.6
C14–C21–N2	178.3(6)	179.8	179.0(5)	179.7
C12–C11–S1–N1	88.7(3)	90.0	37.9(3)	89.1
O1–S1–C11–C12	−26.4(3)	22.9	−81.0(3)	44.4
O1–S1–N1–Cu1	–	–	−175.1(2)	86.1
O2–S1–C11–C16	–	–	−24.8(3)	26.5
O2–S1–N1–Cu1	–	–	−46.1(2)	14.8

Table 3
Selected non-bonded contacts (Å) and angles (°).

	D–H[a]	H···A[a]	D···A[a]	D–H···A[a]
Compound ***1***				
N1–H1···O1^{i}	0.981	1.97	2.931(3)	166.4
C13–H13···N2^{ii}	1.02	2.59	3.565(5)	160.1
Complex ***2***				
N1–H1···O1^{iii}	0.86	2.41	3.039(3)	130.9
N3–H33···O1^{iii}	0.85	2.32	3.119(3)	158.5
N3–H31···O2^{iv}	0.83	2.30	2.936(3)	134.4
N3–H32···O2^{v}	0.89	2.35	3.229(3)	167.6
N3–H32···S1^{v}	0.89	2.81	3.671(3)	161.5

Symmetry codes: (i) $-x+1/2, -y, z-1/2$; (ii) $-x, y-1/2, -z-1$; (iii) $-x+1, -y-1, -z+1$; (iv) $-x+1, -y, -z+1$; (v) $x-1, y, z$
[a] D = C or N and A = N, O, or S.

1560–1500 cm^{-1}, which are assigned to stretching and bending vibrations of the sulfonamide NH_2 groups, respectively. Table 4 shows a shifting of these bands in the complex (see Table 4). The appearance of a new band at 3447 cm^{-1} observed in the IR spectrum of the complex is indicative of the presence of coordinating NH_3 [23,27]. The strong band at 3350 and the doublet at 3268 and 3255 cm^{-1} are due to the asymmetric and symmetric modes of the NH_2 groups. An important feature in the spectrum of the complex is that the band at 3255 cm^{-1} is absent, indicating deprotonation of the amino group.

The strong band at 2228 cm^{-1} in the spectra of the ligand is attributed to ν(CN) vibrations. This band is shifted to 2231 cm^{-1} (calc. 2228 cm^{-1}) and reduce its intensity after complexation. The asymmetric and symmetric modes of SO_2 groups appear at 1332 and at 1096 cm^{-1}, respectively. The asymmetric mode is shifted to 1207 cm^{-1} (calc. 1225 cm^{-1}) and the symmetric one remains almost unchanged in the complex, 1099 cm^{-1} (calc. 1062 cm^{-1}).

In the Raman spectra the asymmetric mode appears at 1334 cm^{-1} and is not observed after complexation. However, the symmetric one is observed at 1092 in the ligand and at 1097 cm^{-1} in the complex. The band at 904 cm^{-1} in the IR spectrum of the ligand and at 900 cm^{-1} in Raman spectrum is attributed to the ν(S–N) vibrations which is shifted to 977 cm^{-1} (986 cm^{-1} in Raman) under complexation. This is in agreement with the shortening of the S–N bond length relative to that of the uncoordinated ligand as was discussed in Section 3.1.

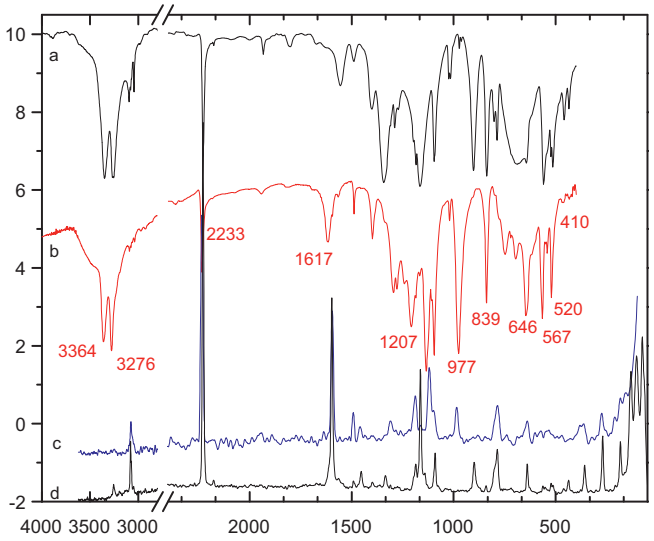

Fig. 4. FTIR and Raman spectra at room temperature. (a) IR spectrum of the free sulfonamide, (b) IR spectrum of the copper complex, (c) Raman spectrum of the copper complex, (d) Raman spectrum of the free sulfonamide.

The nature of the metal–ligand bond is confirmed by the new bands that develop at 410 and 365 cm^{-1} in the IR and Raman spectra of the complex, which are assigned to Cu–NH and Cu–NH_3 vibrations, respectively (calc. 422 and 383 cm^{-1}, correspondingly) [24,31].

3.3.2. Electronic absorption spectra

The electronic absorption spectra of the ligand (1) and complex (2) were first determined in DMSO. However the results obtained for the complex, together with the color change of the solution suggest that it undergoes some decomposition in DMSO. For that reason the spectrum was determined in solid state in KBr pellet. The spectrum of the ligand was determined in the same conditions for consistency.

The spectrum of the ligand (1) shows four intense bands at 245, 273, 282 together with a weak one at 333 nm, (in DMSO the observed bands are: 258, 278, 286 and a weak one at 324 nm). Similar features are displayed in the DMSO calculated spectrum, for the molecule modeled as deprotonated in the sulfonamide end. The intense bands at 286, 278 and 258 nm are in agreement with calculated transitions at 276 (oscillator strength $f = 0.08$), 272 ($f = 0.03$) and 250 nm ($f = 0.12$) assigned to $n \rightarrow \pi^*$, $n \rightarrow \pi^*$ and $\pi \rightarrow \pi^*$ transitions respectively. An additional band is calculated at 322 nm ($f = 0.02$), originated in HOMO–LUMO transitions, for the HOMO centered in the sulfonamide N atom and the LUMO in the benzene moiety. The UV–VIS spectrum of the solid ligand is not easily calculated as the molecule is involved in a network of H-bonded interactions as shown in Fig. 2, characterized by N–H···O bonds with non-bonded H···O distances of 1.968 Å. The associated N–H distance is slightly larger than the average values reported for other sulfonamide complexes (0.981 vs 0.8 Å) [33–35]. These conditions cannot be modeled through the optimization of a single molecule, which does not represent either the periodicity of the solid structure, leading to shorter N–H distances and no H-bonds. An ensemble of two molecules or the modeling of explicit water molecules to mimic the H-bond coordination did not give either the expected result in the calculated spectrum. In all the cases no calculated bands develop before 270 nm. However, the $n \rightarrow \pi^*$ transitions

Table 4
Observed FTIR and Raman bands and calculated IR frequencies and Raman amplitudes, in cm^{-1}, of p-cyanobenzenosulphonamide and copper complex.

Ligand			Complex			Assignments
Infrared	B3LYP	Raman	Infrared	B3LYP	Raman	
			3447 sh	3451		ν_a NH_3
			3380 vs	3392		ν N–H
3350 vs	3493		3364 vs	3386		(ν_a NH_2) ν N–H
3268 vs/3255 vs	3370	3257 vw	3283 vs	3205		(ν_s NH_2) ν N–H
			3276 vs	3187		ν_s NH_3
3096 m	3081	3080 w	3088 w	3116	3078 m	ν C–H
2228 vs	2234	2228 vs	2231 m	2228	2234 vs	ν CN
			1617 m	1620		δ NH_3
1595 m	1568	1597 vs	1597 w	1607	1595 s	ν C–H + ring
1555 m	1528					δ NH_2
1344 s	1365		1338 m	1364		ν C–C
1332 s	1283	1334 vw	1207 m	1225		ν_{as} SO_2 δ NH_2
1288 w	1274		1293 m	1275		ν C–C
1166 s		1163 s	1169 w	1176	1188 m	δ NH_2 + δ NH_3
			1133 s	1139		δ NH_3
1096 s	1084	1092 m	1099 s	1062	1097 sh	ν_s SO_2 + ν C–S + ring
904 s	786	900 m	977 s	855	986 m	ν S–N
839 s		842 vw	839 m	820		Ring
			700 w	706		ω NH_3
645 m	623	639 m	646 m	614	641 m	δ NH + δ NH_3
			600 sh	591		Ring
560 s	600	563 vw	567 s	555		δ SO_2 + ring
524 m	524	524 vw				ρ NH_2
514 m		514 vw	520 s	513		Ring
			410 w	422		ν Cu–NH
435 w		438 m	439 w			Ring
				383	365 w	ν Cu–NH_3
		270 m			276 w	Lattice

should be strongly influenced by the charge density on the sulfonamide N atom, and hence by the N–H distance. As previously shown for the DMSO modeled case, the band ~320 nm is only calculated for the negative species, leading us to assume that at least some NH bonds should be lengthened in the solid phase.

The experimental spectrum of the complex shows a low intensity, broad absorption bands centered at 737 and 592/505 nm (calculated at 732 and 532 nm) originated in a ligand to metal charge transfer transition to the d-centered LUMO orbital. The band at 732 nm is calculated with intensity zero, but can gain intensity through vibronic coupling. Several bands are calculated between 490 and 450 nm, with no intensity, originated in d–d transitions, followed by $n \rightarrow \pi^*$ transitions at 384–380 nm and ligand to metal charge transfer between 354 and 305 nm. Calculated $\pi \rightarrow \pi^*$ transitions start at 295 nm. As for the case of the ligand, the position of the bands can be strongly affected by the structure of the solid (see Fig. 4). This is particularly important for the charge transfer transitions.

4. Conclusions

This study reports the synthesis and characterization of the p-cyanobenzenosulfonamide and a new Cu(II) complex $[Cu(L)_2(NH_3)_2]$. Both compounds were structurally characterized via X-ray crystallography. Their UV, IR and Raman properties are in a good agreement with the X-ray crystallography. B3LYP calculations have been used to compare the structural characteristics and to better assign the spectroscopic features. The agreement with the experimental excitation energies and intensities shows that the theoretical description of the electronic and vibrational structure are essentially correct.

Supplementary data

CCDC 849244 and CCDC 849243 contain the supplementary crystallographic data for **1** and **2** respectively.

These data can be obtained free of charge via http://www.ccdc.ca-m.ac.uk/conts/retrieving.html, or from the Cambridge Crystallographic Data Centre, 12 Union Road, Cambridge CB2 1EZ, UK; fax: +44 1223 336 033; or e-mail: deposit@ccdc.cam.ac.uk.

Acknowledgments

D.B.S., M.E.Ch.V. G.A.E. and P.C. thanks CONICET (CEQUINOR, PIP0356 and PIP 1529), ANPCyT (PME06 2804 and PICT06 2315), SUBCYT and CICPBA, República Argentina, for financial support. G.E.C. thanks to the University of San Luis and G.E. thanks to the Center for Research Computing at the University of Notre Dame.

References

[1] A. Scozzafava, T. Owa, A. Mastrolorenzo, C.T. Supuran, Curr. Med. Chem. 10 (2003) 925.
[2] M.A. Ilies, Metal complexes of sulfonamides as dual carbonic anhydrase inhibitors, in: C.T. Supuran, J.-Y. Winum (Eds.), Drug Design of Zinc–Enzyme Inhibitors: Functional, Structural, and Disease Applications, John Wiley & Sons, Inc., Hoboken, NJ, USA, 2009, pp. 439. http://dx.doi.org/10.1002/9780470508169.ch21.
[3] A. Bult, Met. Ions Biol. Syst. 16 (1983) 261.
[4] M. Dizdaroglu, Free Radic. Biol. Med. 10 (1991) 225.
[5] L.M. Rossi, A. Neves, A.J. Botoluzzi, R. Hörner, B. Szpoganicz, H. Terenzi, A.S. Mangrich, E. Pereira-Maia, E.E. Castellano, W. Haase, Inorg. Chim. Acta 358 (2005) 1807.
[6] CAD4 Express Software, Enraf–Nonius, Delft, The Netherlands, 1994.
[7] K. Harms, S. Wocadlo, XCAD-4, Program for Processing CAD-4 Diffractometer Data, University of Marburg, Germany, 1995.
[8] CrysAlisPro, Oxford Diffraction Ltd., Version 1.171.33.48 (Release 15–09-2009 CrysAlis 171.NET).
[9] G.M. Sheldrick, Acta Cryst. A64 (2008) 112.
[10] A.L. Spek, Acta Crystallogr., Sect. A C34 (1990) 46.
[11] M. Nardelli, J. Appl. Crystallogr. 28 (1995) 659.
[12] M.N. Burnett, C.K. Johnson, ORTEP-III Report ORNL-6895, Oak Ridge National Laboratory, Oak Ridge, Tennessee, USA, 1996.
[13] L.J. Farrugia, WinGX, An Integrate System of Windows Programs for the Solution, Refinement and Analysis of Single Crystal X-Ray Diffraction Data, Dept. of Chemistry, University of Glasgow, 1997–2003.
[14] C.F. Macrae, P.R. Edgington, P. McCabe, E. Pidcock, G.P. Shields, R. Taylor, M. Towler, J. van de Streek, J. Appl. Cryst. 39 (2006) 453.
[15] B. Murphy, B. Hathaway, Coord. Chem. Rev. 243 (2003) 237.

[16] M.J. Frisch, G.W. Trucks, H.B. Schlegel, G.E. Scuseria, M.A. Robb, J.R. Cheeseman, G. Scalmani, V. Barone, B. Mennucci, G.A. Petersson, H. Nakatsuji, M. Caricato, X. Li, H.P. Hratchian, A.F. Izmaylov, J. Bloino, G. Zheng, J.L. Sonnenberg, M. Hada, M. Ehara, K. Toyota, R. Fukuda, J. Hasegawa, M. Ishida, T. Nakajima, Y. Honda, O. Kitao, H. Nakai, T. Vreven, J.A. Montgomery Jr., J.E. Peralta, F. Ogliaro, M. Bearpark, J.J. Heyd, E. Brothers, K.N. Kudin, V.N. Staroverov, R. Kobayashi, J. Normand, K. Raghavachari, A. Rendell, J.C. Burant, S.S. Iyengar, J. Tomasi, M. Cossi, N. Rega, J.M. Millam, M. Klene, J.E. Knox, J.B. Cross, V. Bakken, C. Adamo, J. Jaramillo, R. Gomperts, R.E. Stratmann, O. Yazyev, A.J. Austin, R. Cammi, C. Pomelli, J.W. Ochterski, R.L. Martin, K. Morokuma, V.G. Zakrzewski, G.A. Voth, P. Salvador, J.J. Dannenberg, S. Dapprich, A.D. Daniels, Ö. Farkas, J.B. Foresman, J.V. Ortiz, J. Cioslowski, D.J. Fox, Gaussian 09, Revision *A.02*, Gaussian, Inc., Wallingford, CT, 2009.
[17] A.D. Becke, D.R. Yarkony, Modern Electronic Structure Theory Part II, World Scientific, Singapore, 1995.
[18] L. Radom, P.v.R. Schleyer, J.A. Pople, Ab Initio Molecular Orbital Theory, John Wiley & Sons, New York, 1986.
[19] (a) P.J. Hay, W.R. Wadt, J. Chem. Phys. 82 (1985) 270;
(b) W.R Wadt, P.J. Hay, J. Chem. Phys. 82 (1985) 284.;
(c) P.J. Hay, W.R. Wadt, J. Chem. Phys. 82 (1985) 299.
[20] (a) D.L. Harris, Curr. Opin. Chem. Biol. 5 (2001) 724;
(b) L. Noodleman, T. Lovell, W.G. Han, J. Li, F. Himo, Chem. Rev. 104 (2004) 459;
(c) E.I. Solomon, R.K. Szilagyi, S. DeBeer, G.L. Basumallick, Chem. Rev. 104 (2004) 419;
(d) G. Estiu, K.M. Merz Jr., J. Phys. Chem. B111 (2007) 10263.
[21] F.H. Allen, Acta Cryst. B58 (2002) 380.
[22] I.J. Bruno, J.C. Cole, P.R. Edgington, M. Kessler, C.F. Macrae, P. McCabe, Acta Cryst. B58 (2002) 389.
[23] CCCD, A Program for the Analysis and Display of Data Retrieved from the CSD, Cambridge Crystallographic Data Centre, 12 Union Road, Cambridge, England, 1994.
[24] B. Mennucci, J. Tomasi, R. Cammi, J.R. Cheeseman, M.J. Frisch, F.J. Devlin, S. Gabriel, J. Phys. Chem. A106 (2002) 6102.
[25] G.E. Camí, E.E. Chufán, J.C. Pedregosa, E.L. Varetti, J. Mol. Struct. 570 (2001) 119.
[26] B. Macías, M.V. Villa, E. Fiza, I. García, A. Castiñeiras, M. Gonzalez-Alvarez, J. Borrás, J. Inorg. Biochem. 88 (2002) 101.
[27] B. Murphy, B. Hathaway, Coord. Chem. Rev. 243 (2003) 237.
[28] C. Pedregosa, J. Casanova, G. Alzuet, J. Borrás, S. Garcia-Granda, M.R. Diaz, A. Gutierrez-Rodriguez, Inorg. Chim. Acta 232 (1995) 117.
[29] E. Kremer, G. Facchin, E. Estévez, P. Alborés, E.J. Baran, J. Ellena, M.H. Torre, J. Inorg. Biochem. 100 (2006) 1167.
[30] B. Macías, I. García, M.V. Villa, J. Borrás, M. González-Álvarez, A. Castiñeiras, Inorg. Chim. Acta 353 (2003) 139.
[31] E. Borrás, G. Alzuet, J. Borrás, J. Server-carrió, A. Castiñeiras, M. Liu-González, F. Sanz-Ruiz, Polyhedron 19 (2000) 1859.
[32] M. González-Álvarez, G. Alzuet, J. Borrás, S. García-Granda, J.M. Montejo-Bernardo, J. Inorg. Biochem. 96 (2003) 443.
[33] B. Malika, B. Radia, A. Nour-Eddine, B. Carrole, X-ray Struct. Anal. Online 26 (2010) 13.
[34] M. Mondelli, V. Brune, G. Borthagaray, J. Ellena, O.R. Nascimento, Q. Clarice, C.Q. Leite, A.A. Batista, M.H. Torre, J. Inorg. Biochem. 102 (2008) 285.
[35] C.A. Otter, S.M. Couchman, J.C. Jeffery, K.L.V. Mann, E. Psillakis, M.D. Ward, Inorg. Chim. Acta 278 (1998) 178.